

# Colorimetric and fluorescent TRAP assays for visualising and quantifying fish osteoclast activity

Lalith Prabha Ethiraj,<sup>1</sup> En Lei Samuel Fong,<sup>1</sup> Ranran Liu,<sup>2</sup> Madelynn Chan,<sup>1,3</sup> Christoph Winkler,<sup>2</sup> Tom James Carney<sup>1,4</sup>

<sup>1</sup>Lee Kong Chian School of Medicine, Nanyang Technological University, Singapore

<sup>2</sup>Department of Biological Sciences and Centre for Bioimaging Sciences, National University of Singapore

<sup>3</sup>Department of Rheumatology, Allergy and Immunology, Tan Tock Seng Hospital, Singapore

<sup>4</sup>Institute of Molecular and Cell Biology (IMCB), A\*STAR (Agency for Science, Technology and Research), Singapore

## ABSTRACT

Histochemical detection of tartrate-resistant acid phosphatase (TRAP) activity is a fundamental technique for visualizing osteoclastic bone resorption and assessing osteoclast activity status in tissues. This approach has mostly employed colorimetric detection, which has limited quantification of activity *in situ* and co-labelling with other skeletal markers. Here, we report simple colorimetric and fluorescent TRAP assays in zebrafish and medaka, two important model organisms for investigating the pathogenesis of bone disorders. We show fluorescent TRAP staining, utilising the ELF97 substrate, is a rapid, robust, and stable system to visualise and quantify osteoclast activity in zebrafish, and is compatible with other fluorescence stains, transgenic lines and antibody approaches. Using this approach, we show that TRAP activity is predominantly found around the base of the zebrafish pharyngeal teeth, where osteoclast activity state appears to be heterogeneous.

**Key words:** TRAP; tartrate-resistant acid phosphatase; osteoclast; ELF97; fracture; zebrafish; medaka.

**Correspondence:** Tom James Carney, Lee Kong Chian School of Medicine, Experimental Medicine Building, Yunnan Garden Campus, 59 Nanyang Drive, Nanyang Technological University, 636921 Singapore.  
E-mail: tcarney@ntu.edu.sg

**Ethics approval:** All investigations were carried out in accordance with approved IACUC protocols (A18002) at Nanyang Technological University, Singapore.

**Contributions:** All the authors made a substantive intellectual contribution. All the authors have read and approved the final version of the manuscript and agreed to be accountable for all aspects of the work.

**Conflict of interest:** The authors declare that they have no competing interests, and all authors confirm accuracy.

## Introduction

Bone remodeling is a normal physiological process for maintenance of bone mineral density, which is accomplished by harmonized function of osteoclasts and osteoblasts. Osteoclasts are responsible for removal of bone, whereas the osteoblasts carry out new bone formation.<sup>1</sup> Disruption of the balance between osteoclastic bone resorption and osteoblastic bone formation can be seen in various bone diseases such as Osteogenesis imperfecta, osteoporosis, metastatic cancer and Paget's disease.<sup>2</sup> Accordingly, observation of osteoclast number and activity *in situ* is a critical tool in assessing the pathogenesis of skeletal disease. Osteoclasts are generated from the myeloid lineage under the influence of macrophage colony-stimulating factor (M-CSF) and its receptor, Csf1r,<sup>3,4</sup> whilst osteoclasts can be activated by binding of receptor for activation of nuclear factor kappa B (NF- $\kappa$ B) ligand (RANKL) to its receptor RANK.<sup>5,6</sup>

Once activated, osteoclasts express tartrate-resistant acid phosphatase (TRAP or TRAcP), encoded by the *ACP5* gene, which is involved in hydrolysis of bone matrix,<sup>7</sup> and its activity can be used as a proxy of osteoclastic bone resorption activity.<sup>8</sup> The phosphatase activity of TRAP forms the basis of its histological detection. Presence of the enzyme within a sample removes phosphate from an inert naphthol AS-BI phosphate substrate, which then is able to conjugate with a diazonium salt to form a red precipitate. This colorimetric reaction can thus be visualized by light microscopy. TRAP is resistant to tartrate inhibition, distinguishing it from alkaline phosphatases of other cells *in vivo*.<sup>8</sup>

A fluorescence-based staining method has also been developed for detection of TRAP activity.<sup>9</sup> This employs the ELF97 substrate which yields a brightly fluorescent precipitate upon removal of a phosphate group by a phosphatase. The dephosphorylated product is maximally excited at 360 nm while emission occurs maximally at 530 nm. Such a long Stokes shift reduces interference caused by autofluorescence or other stains and greatly expands its ability to combine with other fluorescent labels.<sup>10,11</sup>

Fish species are increasingly being used as models of bone disease and to study the biology of the skeletal system, as they show a strong conservation of genetic control of bone homeostasis.<sup>12</sup> Here, we describe protocols and applicability of colorimetric and ELF97 based TRAP assays in zebrafish and medaka. We show the versatility that a fluorescent based TRAP staining approach provides to visualize osteoclast activity in fish.

## Materials and Methods

### Fish husbandry

Adult zebrafish were used at 4 months of age and were maintained in a recirculation system at the Nanyang Technological University Zebrafish Facility at 28°C with a 14- and 10-h light and dark cycle. All investigations were carried out in accordance with approved IACUC protocols (A18002) at Nanyang Technological University. The AB wild type strain was used for most experiments, whilst the *csf1rq<sup>del</sup>* (*panther*) mutant strain was used to genetically deplete osteoclasts. Labelling of osteoclasts and osteoblasts employed the *ctsk:dsred*; *sp7:egfp* transgenic zebrafish.<sup>13</sup> Transgenic *rankl:HS:cfp* medaka used were reared in the fish facility at the Department of Biological Sciences, National University of Singapore, under the IACUC protocols (BR19-0120, R18-0562). Medaka larvae were heat shocked at 9 days post fertilisation (dpf) in a 39°C water bath for 2 h. All embryos were

obtained from natural crosses. Zebrafish embryos were raised at 28°C in E3 medium (5 mM NaCl, 0.17 mM KCl, 0.33 mM CaCl and 0.33 mM MgSO<sub>4</sub>) and medaka embryos were raised at 30°C in medaka medium (19.3 mM NaCl, 0.23 mM KCl, 0.13 mM MgSO<sub>4</sub>, 0.2 mM Ca(NO<sub>3</sub>)<sub>2</sub>, 1.7 mM HEPES, pH 7.0) until 12dpf. Adult and larval fish were anaesthetised using 0.02% Tricaine (A5040, Sigma-Aldrich, St. Louis, MO, USA) buffered to pH7.0 with Tris. Fish were euthanised using immersion in 0.4% Tricaine (pH 7.0).

### Bisphosphonate treatment of zebrafish

Adult fish were treated with 100  $\mu$ g/mL alendronate solution obtained by dissolving alendronate (A4978, Sigma-Aldrich) in fish tank water. The 12 dpf zebrafish larvae were treated using 40  $\mu$ g/mL alendronate solution dissolved in E3 medium. For treatment of adults, fish were immersed in the drug solution for 24 h once a week for 5 weeks. Following each exposure pulse, treated fish were placed in a tank of fresh tank water for 2-day recovery, and then returned to the flow racks until the next exposure cycle. Larvae were treated by single immersion in the drug solution for 14 h immediately before experiments.

### Zebrafish jaw and pharyngeal teeth dissection

To extract the teeth bearing fifth ceratobranchial bone, adults were euthanised and laid laterally on a Petri dish under a dissecting microscope. Drummond number 5 Watchmaker's forceps were inserted from a posterior angle under the operculum, and the bony structure just below the gills were extracted out, together with the surrounding soft tissue. Tissues were lightly dissected away from the bone manually using Watchmaker's forceps and Vannas microsurgical scissors. Specimens were then processed by staining and then placed on a glass slide for imaging under a Zeiss dissecting fluorescent or confocal microscope.

### Fish tail fin ray fractures

After anaesthetisation, adult zebrafish were positioned laterally under a dissecting stereomicroscope with tail spread out. Paper tissue was used to remove excess water. A fin ray was fractured by crush injury at the centre of a ray segment using forceps (Drummond number 5) according to Tomecka *et al.*<sup>14</sup> Up to four crushes were made per fin on non-adjacent fin rays and care was taken not to impact the neighbouring tissues. After injury, fish were transferred to a quiet tank for brief recovery. After the stipulated crush healing duration, the whole tail fin was dissected using a scalpel under anaesthetic, and the isolated tail fin subjected to staining and imaging.

### Tissue fixation

Prior to staining, all tissues and larvae were fixed in 4% paraformaldehyde (PFA) (P6148, Sigma-Aldrich) in phosphate buffered saline (PBS) on a rotator for 40 min to 4 h at room temperature. The 4% PFA was removed from the samples with three washes of PBSTriton [0.1% Triton-X-100 (H5141, Promega Co., Madison, WI, USA) in 1x PBS] for 5 min each at room temperature, and then processed for TRAP staining.

### Colorimetric TRAP staining

The colorimetric TRAP staining protocol was adapted from Takahashi *et al.*<sup>15</sup> Briefly, 5 mg of Naphthol AS-MX phosphate (N4875, Merck, Darmstadt, Germany) was dissolved in 0.5 mL of N, N'-dimethylformamide (D4451, Merck) to make a 10 mg/mL naphthol AS-MX phosphate "Solution A" stock. A "Solution B" stock solution of 50 mM sodium tartrate and 1.6 mM Fast Red Violet LB was made by dissolving 0.575 g of sodium L-tartrate dibasic dihydrate (228729, Merck) in 50 mL of 0.1M sodium acetate buffer (adjusted to pH 5.0 with 100% acetic acid), and then

adding 30 mg Fast Red Violet LB salt (F3381, Merck).

TRAP staining solution was obtained by mixing 1 part Solution A to 100 parts Solution B together (e.g., 0.5 mL Solution A was added to 50 mL Solution B). This final solution can be stored for 1 month at 4°C.

Following fixation and washing, the final PBSTriton wash was replaced with 1 mL of TRAP staining solution and samples incubated at room temperature for 3 h in the dark. Samples were then washed with PBST (0.1% Tween in PBS) three times at room temperature and then re-fixed with 4% paraformaldehyde for 30 min.

### Sample bleaching

If samples needed to be bleached to remove pigment following colorimetric TRAP staining, they were washed three times in PBST for 5 min each following re-fixing, and a bleach solution (0.5% KOH and 3% H<sub>2</sub>O<sub>2</sub> final concentrations) added. Samples were bleached at room temperature for 20 min with tube lids left open. Bleach solution was removed with thorough washing in PBST. Stained samples were washed into 90% glycerol for imaging and long-term storage in the dark at 4°C.

### Fluorescence TRAP staining protocol

The fluorescent TRAP staining approach was adapted from Filgueira.<sup>9</sup> Briefly, fluorescent ELF97-TRAP staining solution of 50 mM sodium tartrate and 0.2 mM ELF97 was made by dissolving 0.575 g of sodium L-tartrate dibasic dihydrate in 50 mL of 0.1 M sodium acetate buffer (pH 5.0), and then adding 20 µL 5mM ELF97 stock solution (E6589, Thermo Fisher Scientific, Waltham, MA, USA). Following fixation and PBSTriton washing, the final PBSTriton wash was removed, and the samples then incubated in fluorescent TRAP staining solution for 2 h at room temperature. Specimens were washed three times with PBST for 5 min each, followed by re-fixation with 4% PFA for 30 min at room temperature. Samples were again washed three times in PBST before transferring to 90% glycerol for imaging and storage, or for additional fluorescent staining approaches.

### Combined ELF97 fluorescence staining protocol

Generally, for all combinatorial ELF97 and fluorescent labelling, ELF97 staining was performed first, and the second staining approach initiated after the re-fixation step. For DAPI counter staining, samples were washed out of PFA with three 5 min washes of PBST, followed by 30 min incubation in 5 µg/mL DAPI (4',6-diamidino-2-phenylindole) in PBST for 30 min. Samples were rewashed in PBST before transferring to 90% glycerol. For calcified tissue staining, the above was repeated but DAPI was replaced with 0.01% Calcein (C0875, Sigma-Aldrich) in PBST or 0.01% Alizarin Red (A5533, Sigma-Aldrich) in PBST. For immunofluorescent staining following ELF97-TRAP, samples were washed three times in PBST after re-fixing or glycerol storage and then subjected to -20°C acetone for 20 min to permeabilise. Methanol must not be used. Following three washes in PBSTriton samples were incubated in blocking solution for 2-3 h room temperature (4% BSA, 1% DMSO, 0.5% Triton-X-100 in PBS) and immunostaining performed as per Asharani *et al.*<sup>16</sup> and Lee *et al.*<sup>17</sup> Primary antibodies used were chicken anti-GFP (Ab16901, Millipore, MA, USA) at 1:500 and rabbit anti-DsRed (#632496, BD Biosciences, Franklin Lakes, NJ, USA) at 1:200. Secondary antibodies used were Alexa488 goat anti-chicken (A11039, Invitrogen, Waltham, MA, USA) at 1:1000 and Alexa568-goat anti-rabbit (A11011, Invitrogen) at 1:200. Lastly, following secondary antibody staining, specimens were washed three times in PBSTriton for 30 min each and imaged and stored under 90% glycerol at 4°C without exposure to light.

### Cryosectioning

For fluorescent TRAP staining, cryosectioning was performed after the completion of all staining protocols. Samples stained with ELF97, with or without other fluorescent stains, were washed from PBST and mounted into OCT (Tissue-Tek Optimal Cutting Temperature freezing compound; Sakura Finetek, Torrance, CA, USA) and orientated in cryomolds (Tissue Tek Cryomold, Sakura Finetek). These were flash frozen in liquid nitrogen or through storage in a -80°C freezer. 20 µm cryosections were made using Leica Cryostat (CM 3050). Sectioned fluorescent samples on slides were dried for at least 1 h at room temperature or on a 42°C heat block. They were then washed with PBS, re-dried overnight at room temperature, and then covered in Vectashield mounting medium under a coverslip and imaged. For colorimetric TRAP staining, cryosectioning was performed before the TRAP staining protocol. After PFA fixation, samples were washed in PBS at 4°C overnight, and then substituted in 5, 10, 15 and 30% sucrose/PBS solution, for 30 min each. Finally, samples were exchanged into 30% sucrose:OCT at 1:1 for 30 min and in 100% OCT overnight. Samples were mounted in cryomolds and frozen. 20 µm cryosections were made on a Leica cryostat, and the slides dried overnight. Prior to beginning the colorimetric TRAP staining, slides were washed in 100% methanol for 10 min and then PBS, and finally subjected to the colorimetric TRAP staining protocol. For medaka fin sections, dissected fins were washed with PBST for three times and mounted in 1.5% low melting agarose (LMA), 5% sucrose in PBS and soaked in 30% sucrose at 4°C overnight. Samples were mounted in cryomolds, frozen and 20 µm cryosections were made on a Leica cryostat. Slides were dried for 1 h at room temperature. Slides were then washed for three times in PBST before proceeding to TRAP staining.

### Imaging

Samples were visualised using widefield Colibri on an AxioImager M2 (Zeiss Jena, Germany), or confocal fluorescent microscopy (Zeiss LSM800) and processed using Zen software (Zeiss) or Fiji (ImageJ, ver. 1.52p). For the ELF97 crush injury time series assay, corrected total crush fluorescence was used to measure fluorescent signal emitted.<sup>14,18</sup> All measurements were normalised against fluorescence detected at an unfractured site. For ELF97 detection, samples were illuminated with 405 nm wavelength laser, and the emission detected using a filter collecting between 564 nm – 617 nm. For the Colibri system, samples were illuminated with the 385nm LED, and the mCherry Filter Cube used as the emission filter.

### Statistics

Statistical analysis was performed using Prism GraphPad software. ANOVA with either Bonferroni or Tukey post-tests were used.

## Results

### A colorimetric TRAP staining approach to detect osteoclastic activity in zebrafish and medaka

We evaluated our colorimetric TRAP staining method using a zebrafish tail fin crush injury model.<sup>14</sup> We saw that TRAP staining is exclusive to fracture sites at 4 days post crush (4 dpc) and not in adjacent unfractured rays (Figure 1A). We demonstrated that this staining of fractured fin rays was indeed reporting osteoclastic TRAP activity as it was largely abolished in the osteoclast deficient *csf1ra*<sup>je1</sup> mutant (Figure 1B).<sup>19,20</sup> Our colorimetric method also detected TRAP activity at the fifth ceratobranchial bone in

12dpf larvae, where specific osteoclast TRAP activity around the pharyngeal teeth is well known to occur.<sup>21,22</sup> No TRAP positive staining around the pharyngeal teeth regions were observed in the *csfr1a<sup>4e1</sup>* mutants as expected,<sup>13</sup> nor was any staining noted in other pharyngeal bones of wild-type (WT) controls, confirming the activity to be associated only with osteoclastic activity in teeth bearing elements of 12dpf larvae (Figure 1 C,D). Finally, we wanted to confirm the applicability of our staining protocol to other fish species. We used medaka which had osteoclast activity primed by two methods. Firstly, we amputated adult tail fins and performed

colorimetric TRAP staining on cryosections either immediately (0 days post amputation, dpa; Figure 1E) or after 6 days of regeneration (6dpa; Figure 1F). TRAP activity was found in the blastema region, near segments after 6 days, suggesting that osteoclasts were active in the regenerating fins after regeneration had progressed (Figure 1E, F). Secondly, we used a transgenic approach to trigger ectopic osteoclast formation at 12dpf through heat-shock induced expression of a Rankl transgene.<sup>23,24</sup> 9dpf *rankl:HS:cfp* medaka larvae were heat shocked for 2 h at 39°C and TRAP staining performed on cryosections 3 days post heat-shock.

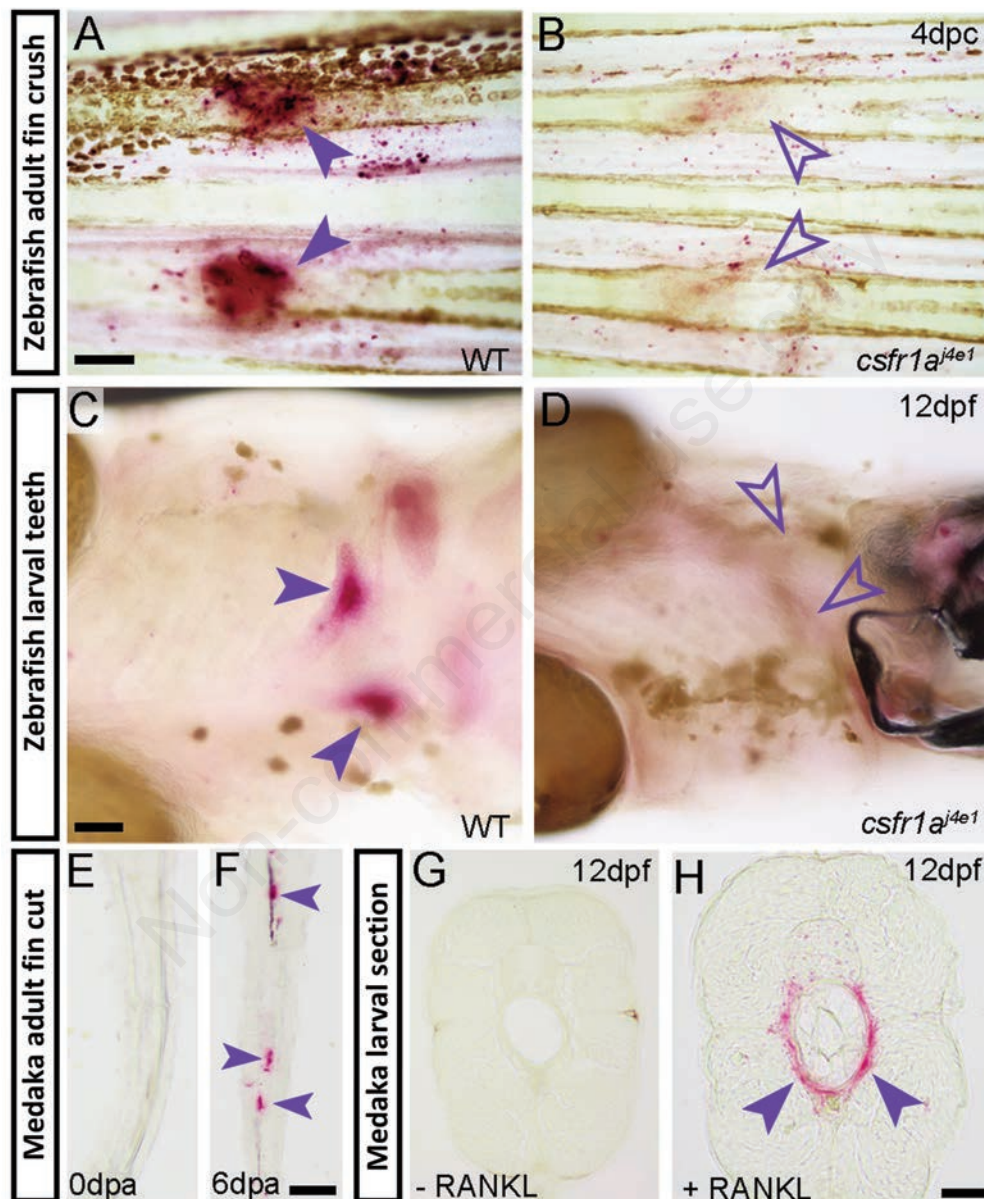


**Figure 1.** Identification of activated osteoclasts using conventional TRAP stain. A-H) Brightfield images of zebrafish (A-D) and medaka (E-H) adult fins (A-B,E,F), or 12dpf larvae (C,D,G H) processed by colorimetric TRAP staining. Individuals are either wild-type (WT; A, C, E, F), homozygous *csfr1a<sup>4e1</sup>* mutants (B,D) or transgenic for *rankl:HS:cfp* (G,H). Images are of whole-mount fins at 4 dpc (A,B), whole-mount ventral views (C, D) or longitudinal (E) or transverse cryosections (G,H). Fins in (E,F) have been amputated and stained immediately (0dpa; E) or after 6 days (dpa; F). The larva in (H) has been subjected to heat shock to express RANKL, while the larva in (G) was not heat shocked. Red precipitate (blue arrowheads) indicates TRAP locations at fractures (A), pharyngeal teeth of the fifth ceratobranchial bone (C), in regenerating fin rays at 6 days post amputation (6dpa; F) or around notochord in larvae with excess RANKL induced by heat shock (H). TRAP staining is absent when there is no RANKL overexpression (G), at the start of fin regeneration (0dpa; E) or following genetic ablation of osteoclasts (B, D; open blue arrowheads), indicating specificity. Scale bars: A) 200 µm; C) 100 µm; F,H) 50 µm.

*rankl:HS:cfp* larvae showed high osteoclast activity around the notochord (Figure 1H), but this was absent in larvae without heat shock (Figure 1G), in line with the previously shown increase in ectopic osteoclast numbers at this site following Rankl induction.<sup>24</sup> Thus, the colorimetric TRAP staining approach offers a simple cheap method for defining osteoclast activity in fish species in both whole-mount and following cryosections.

### Application of a fluorescent TRAP staining approach to zebrafish

Zebrafish are highly amenable to fluorescent microscopy

approaches. We tested if a described fluorescent TRAP staining approach could be adapted to zebrafish. We tested the ELF97 substrate initially in the tail fin crush injury model. As with the colorimetric assay, we observed a strong fluorescent signal at 3 dpc in fractured rays only and not in adjacent intact rays (Figure 2A). We again showed that this signal was osteoclast dependent as it was absent in *csfr1a*<sup>4e1</sup> mutants and in fish treated for 14 h prior to crushing with 100 µg/mL of the bisphosphonate (BP), alendronate, which acts as an osteoclast poison (Figure 2 B,C). We followed a time course of healing under the three conditions and saw that TRAP staining persisted in the WT crush at 7 and 14 dpc but had

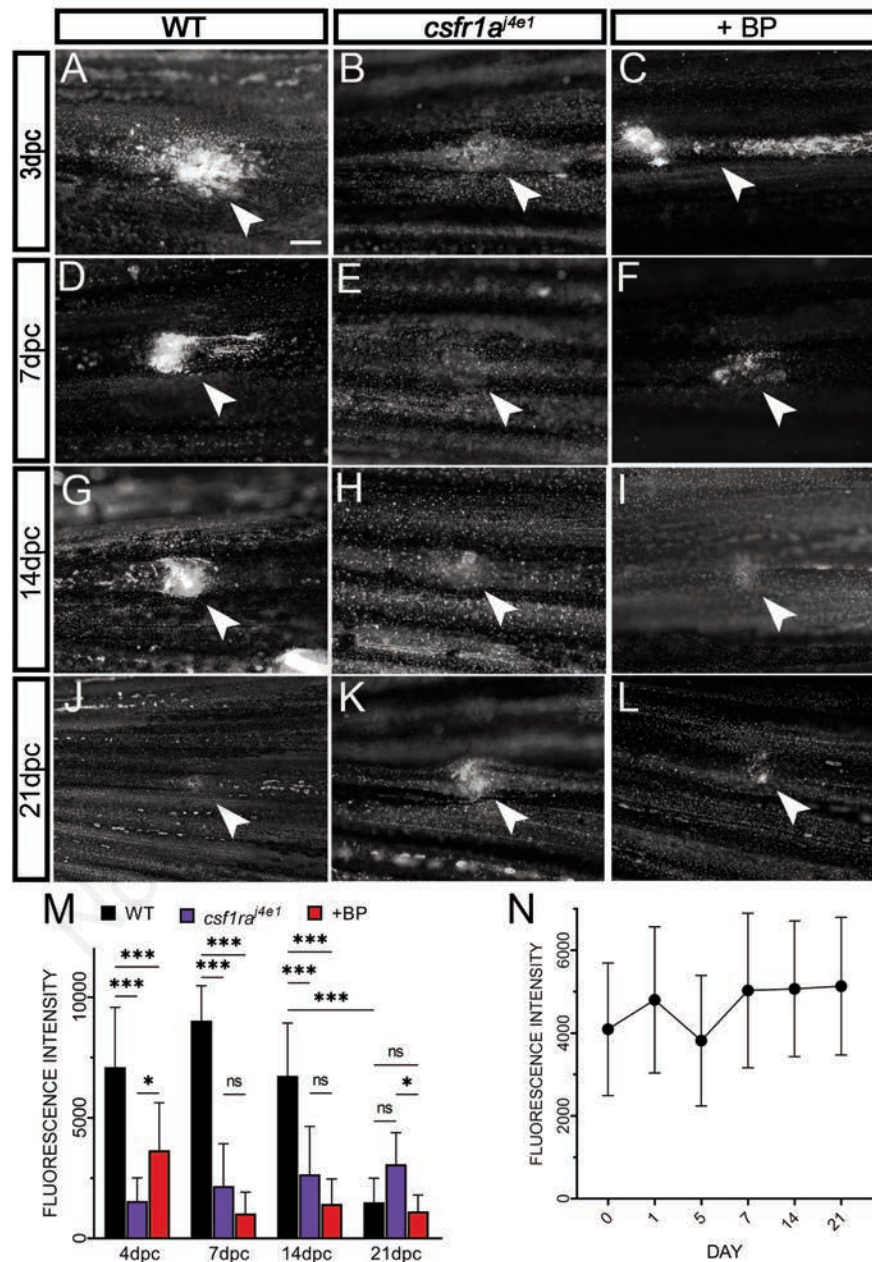


**Figure 2.** A fluorescent TRAP method labels osteoclast activity in zebrafish bone fractures. A-L) Whole-mount widefield fluorescent images of adult fin ray fractures processed for ELF97 fluorescence. Fins were fixed at 3 dpc (A-C), 7 dpc (D-F), 14 dpc (G-I) and 21 dpc (J-L), and were either WT (A,D,G,J), homozygous *csfr1a*<sup>4e1</sup> mutants (B, E, H, K) or treated with 100 µg/mL bisphosphonate (+BP; C, F, I, L). M: Mean fluorescence of crush sites at given timepoints and under the three conditions. \*\*\*= p<0.001, \*=p<0.05, (ANOVA with Bonferroni multiple comparisons test, n=12). N: Mean ELF97 fluorescence at the crush sites of 1 dpc WT zebrafish following storage for 0, 1, 5, 7, 14, 21 days. There was no statistically significant variation over the course of 21 days of storage compared against initial staining (ANOVA, Tukey's multiple comparisons test, n=12). Scale bar: A) 100 µm.

largely resolved by 21dpc (Figure 2 D,G,J), whilst it was mostly absent at all stages in the two osteoclast deficient scenarios (Figure 2 E,F,H,I,K,L). Being a fluorescent stain, ELF97 facilitated quantification of TRAP activity *in situ* (Figure 2M). Mean fluorescence detected in *csf1ra<sup>4e1</sup>* mutants and BP fractures were noted both to be significantly reduced at 4, 7 and 14 dpc compared to WT (Figure 2 A-I, M). At 21 dpc, fluorescence in WT was significantly reduced compared to the previous timepoints (Figure 2 G,J,M). At 21dpc, mean fluorescence in *csf1ra<sup>4e1</sup>* mutant fractures was significantly more than following BP treatment (Figure 2 K,L,M). Statistical trends observed are in agreement with previous observations of osteoclast activity in fractures.<sup>14</sup> However, ELF97 fluorescent imaging made quantification far less subjective and markedly improved analysis throughput. To determine if ELF97 stained samples can be imaged at later dates, we assessed the stability of TRAP fluorescence reaction product after storage. WT tail fins which had been fractured were fixed after 1 day and processed using the ELF97 TRAP staining protocol. They were then stored in the dark at 4°C under glycerol and imaged repeatedly using confocal microscopy at timepoints 0, 1, 5, 7, 14 and 21 days after staining. The mean fluorescence of TRAP staining at the fractures showed no statistically significant change in intensity over the 21 days of storage, indicating stability of ELF97 fluorescence (Figure 2N).

### Fluorescent TRAP staining is compatible with fluorescent protein imaging and fluorescent nuclei and bone staining

Fluorescent microscopy provides the ability to image multiple fluorescent labels simultaneously, facilitating co-localisation studies. The large Stokes shift of ELF97 obviates interference with standard fluorophore spectra. Thus, we assessed if we could combine ELF97 TRAP staining with well used transgenic markers of the zebrafish skeletal system. In particular, the cathepsin K (*ctsk*) gene is expressed in osteoclasts, whilst the *sp7* (= *osterix*, *osx*) transcription factor is expressed in osteoblasts. The promoters of these genes have been used to label these cells with fluorescent proteins in transgenic fish. We performed tail fin ray fractures on *ctsk:dsred; sp7:egfp* double transgenic adults. At 7 dpc, tails were briefly fixed and processed for ELF97 TRAP staining and then counterstained with DAPI. Confocal microscopy of the fracture site of the fin rays revealed that the ELF97 fluorescence co-localised within the field of osteoclast-specific DsRed fluorescence, which appeared at the fracture site (Figure 3 A,B,D-F). Osteoblast-specific green fluorescent protein (GFP) was noted most prominently in the peripheral bone but also showed localised staining within the fracture (Figure 3C).

To assess if our fluorescent TRAP staining approach was compatible with fluorescent bone stains, we used ELF97 in combination with Calcein in whole-mount staining of adult fin ray fractures (Figure 3 G-I) and with Alizarin red in cryosections of the adult pharyngeal teeth where there is continual osteoclast activity (Figure 3 J-L). In the former, ELF97 staining was seen again within parts of the fracture callus, whilst in the cryosections, calcified enamel lamellae of the teeth were circumscribed by osteoclast active regions. TRAP staining localisation around the base of each Alizarin stained tooth matched the pattern seen with colorimetric TRAP and Alizarin staining (Figure 3 M,N). Unlike the conventional TRAP stain combined with Alizarin red cryosections (Figure 3 M,N), ELF97 sections enable differentiation of teeth morphology from osteoclastic activity and also allow comparison of them in a single imaging panel.

### ELF97 allows combination with immunofluorescent staining

In many samples, residual fluorescence from the *ctsk:dsred; sp7:egfp* double transgenes was not visible following TRAP staining. In these cases, it was necessary to detect DsRed and EGFP by immunostaining. To assess if the ELF97 protocol was indeed compatible with immunostaining, we isolated the fifth ceratobranchial bone of *ctsk:dsred; sp7:egfp* double transgenic adults by dissection and fixed overnight in 4% PFA. Following this, there was no observable DsRed or EGFP fluorescence remaining. We performed ELF97 TRAP staining on the samples and then immunofluorescently labelled them using antibodies against DsRed and EGFP. We imaged them in whole-mount and additionally cryosectioned them to ascertain if the labels remained. We saw that the TRAP staining was not disrupted by the immunofluorescent protocol, and that ELF97 was compatible with antibody detection of DsRed and EGFP, both in whole-mount (Figure 4 A-F) and in cryosections (Figure 4 G-L). EGFP signal could be seen in the pulp, dentine and bone of attachment, previously shown as expression domains of *sp7* (Figure 4 A,E,F,G,K,L).<sup>25</sup> The expression domain of EGFP was quite distinct from that corresponding to DsRed, which was predominantly found in the bone regions below each tooth and around the base, indicating distinct localisation of osteoclasts and osteoblasts (Figure 4 B,D,E,F,I-L). ELF97 signal was found in a domain largely overlapping the DsRed domain, although the overlap was not identical, and there were clear locations where osteoclasts were not positive for the TRAP stain and others where the TRAP stain was broader than the DsRed staining (Figure 4 C,D,H,J). Thus, it appears there is heterogeneity of osteoclast state around the base of each tooth in zebrafish, and on the bone itself.

### Discussion

We have shown that ELF97 offers a simple, reproducible, stable, versatile, and quantifiable substitute to conventional colorimetric TRAP stains for analysis of fish osteoclast activity. We have shown that it recapitulates colorimetric TRAP staining in fin fractures and is associated with the fifth ceratobranchial bone which bears the teeth. ELF97 is unusual as it has a large Stokes shift, having maximal excitation at 345 nm and emission at 580 nm. We found a 405 nm laser effective for excitation if a 355 nm UV laser is not available. The recent development of Colibri style LED illumination systems permits use on widefield fluorescent microscopes, as excitation can be tuned and can be uncoupled from the emission filter set. This large Stokes shift provides great versatility when used with other fluorescent channels, and it does not interfere with the detection of other fluorophores. This means ELF97 TRAP staining can be combined with other fluorescent dyes, mineral stains, fluorescent proteins and immunofluorescence, and is compatible with both whole-mount and cryosectioning. Since zebrafish is a polyphyodonty,<sup>26</sup> there is continuous shedding of teeth throughout their life cycle. This provides an excellent model to study spontaneous continuous osteoclastic activity, which can be demonstrated using the ELF97 fluorescent stain. Through combining this stain with other fluorescence staining approaches, we have identified that TRAP activity is not entirely concordant with the presence of osteoclasts in the tooth region or in fractures, but appears to only partially overlap. This highlights the utility of assessing osteoclast activity in conjunction with their location and

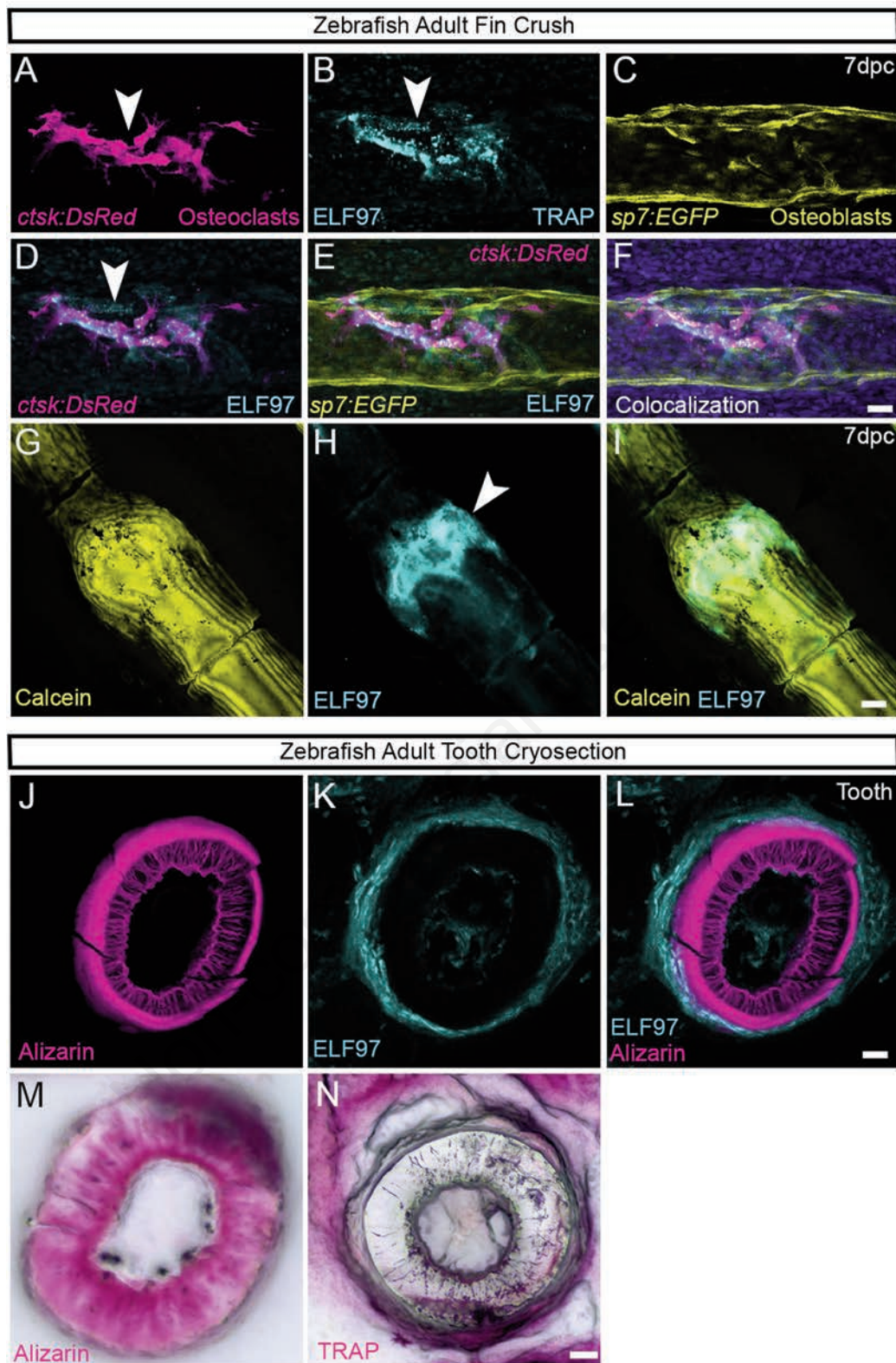


**Figure 3.** Colocalization of TRAP-ELF97 reaction product with fluorescent proteins and dyes. A-F) Whole-mount confocal images of a fin ray fracture in *ctsk:Dsred*; *sp7:egfp* double transgenic adults, processed at 7 dpc for ELF97 TRAP fluorescence and counterstained with DAPI. Individual fluorescent channels for *ctsk:Dsred* (A), ELF97 (B), *sp7:egfp* (C), DsRed and ELF97 channel overlay (D), DsRed, EGFP and ELF97 channel overlay (E), all channels including DAPI (F). TRAP-ELF97 fluorescence is seen associated with DsRed labelled osteoclasts within the callus. G-I) Confocal images of whole-mount adult zebrafish fin ray subjected to crush fracture and processed at 4 dpc for Calcein (G) and ELF97 (H) staining. TRAP activity is seen within the bone matrix of the callus (I). J-N) Confocal image of cryosection through an adult zebrafish pharyngeal tooth which has been stained with Alizarin Red (J,M), ELF97 (K) and colormetric TRAP (N). Overlay of both channels indicates TRAP staining surrounding the bone mineral (L). Scale bars: F,I,L,N) 20  $\mu$ m.

morphology. With fish systems providing increasingly sophisticated models of skeletal diseases, such methodologies will complement the growing array of genetic and labelling resources available.

## Acknowledgments

We thank Dr. Matthew Harris, Department of Genetics, Harvard Medical School, Boston for gifting us the *ctsk:dsred*; *sp7:egfp* double transgenic line.

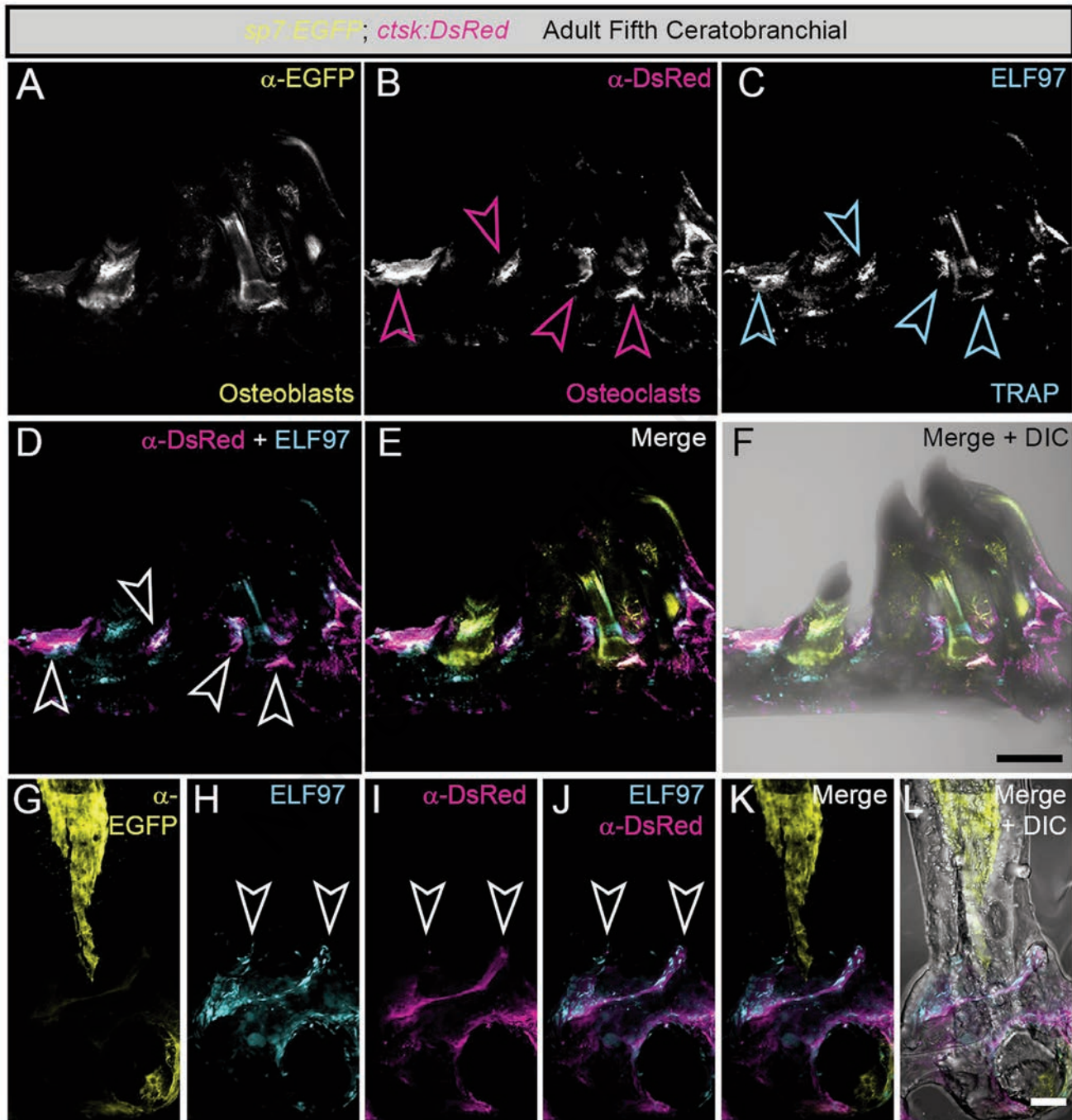


**Figure 4.** Fluorescent TRAP staining can be combined with immunofluorescence. A-L) Confocal images of dissected fifth ceratobranchial bone with pharyngeal teeth of a *ctsk:DsRed*; *sp7:EGFP* double transgenic adult which had been processed for ELF97 TRAP staining (C,H) and immunostained with antibodies against EGFP (A,G) and DsRed (B,I). Both whole-mount (A-F) and cryosectioned (G-L) samples are presented. Co-localisation demonstrates ELF97 signal associated with DsRed positive osteoclasts at the base of the teeth (D,E,J,K), whereas eGFP positive osteoblasts are found within the teeth (E, F, K, L). Fluorescent channels are also shown with DIC image (F,L). Scale bars: F) 200  $\mu$ m; L) 50  $\mu$ m.

## References

- Hattner R, Epker BN, Frost HM. Suggested sequential mode of control of changes in cell behaviour in adult bone remodelling. *Nature* 1965;206:489-90.
- Novack DV, Teitelbaum SL. The osteoclast: friend or foe? *Annu Rev Pathol* 2008;3:457-84.
- Fujikawa Y, Sabokbar A, Neale SD, Itonaga I, Torisu T, Athanasou NA. The effect of macrophage-colony stimulating factor and other humoral factors (interleukin-1, -3, -6, and -11, tumor necrosis factor-alpha, and granulocyte macrophage-colony stimulating factor) on human osteoclast formation from circulating cells. *Bone* 2001;28:261-7.
- Udagawa N, Takahashi N, Akatsu T, Tanaka H, Sasaki T, Nishihara T, et al. Origin of osteoclasts: mature monocytes and macrophages are capable of differentiating into osteoclasts under a suitable microenvironment prepared by bone marrow-derived stromal cells. *Proc Natl Acad Sci USA* 1990;87:7260-4.
- Feige U. Osteoprotegerin. *Ann Rheum Dis* 2001;60:iii81-4.
- Lacey DL, Timms E, Tan HL, Kelley MJ, Dunstan CR, Burgess T, et al. Osteoprotegerin ligand is a cytokine that regulates osteoclast differentiation and activation. *Cell* 1998;93:165-76.
- Kirstein B, Chambers TJ, Fuller K. Secretion of tartrate-resistant acid phosphatase by osteoclasts correlates with resorptive behavior. *J Cell Biochem* 2006;98:1085-94.
- Frith JC, Monkkonen J, Blackburn GM, Russell RG, Rogers MJ. Clodronate and liposome-encapsulated clodronate are metabolized to a toxic ATP analog, adenosine 5'-(beta, gamma-dichloromethylene) triphosphate, by mammalian cells in vitro. *J Bone Miner Res* 1997;12:1358-67.
- Filgueira L. Fluorescence-based staining for tartrate-resistant acidic phosphatase (TRAP) in osteoclasts combined with other fluorescent dyes and protocols. *J Histochem Cytochem* 2004;52:411-4.
- Paragas VB, Kramer JA, Fox C, Haugland RP, Singer VL. The ELF -97 phosphatase substrate provides a sensitive, photo-stable method for labelling cytological targets. *J Microsc* 2002;206:106-19.
- Larison KD, BreMiller R, Wells KS, Clements I, Haugland RP. Use of a new fluorogenic phosphatase substrate in immunohistochemical applications. *J Histochem Cytochem* 1995;43:77-83.
- Dietrich K, Fiedler IA, Kurzyukova A, Lopez-Delgado AC, McGowan LM, Geurtzen K, et al. Skeletal biology and disease modeling in zebrafish. *J Bone Miner Res* 2021;36:436-58.
- Caetano-Lopes J, Henke K, Urso K, Duryea J, Charles JF, Warman ML, et al. Unique and non-redundant function of csf1r paralogs in regulation and evolution of post-embryonic development of the zebrafish. *Development* 2020;147:dev.181834.
- Tomecka MJ, Ethiraj LP, Sanchez LM, Roehl HH, Carney TJ. Clinical pathologies of bone fracture modelled in zebrafish. *Dis Model Mech* 2019;12: dmm.037630.
- Takahashi N, Udagawa N, Kobayashi Y, Suda T. Generation of osteoclasts in vitro, and assay of osteoclast activity. *Methods Mol Med* 2007;135:285-301.
- Asharani PV, Keupp K, Semler O, Wang W, Li Y, Thiele H, et al. Attenuated BMP1 function compromises osteogenesis, leading to bone fragility in humans and zebrafish. *Am J Hum Genet* 2012;90:661-74.
- Lee RT, Knapik EW, Thiery JP, Carney TJ. An exclusively mesodermal origin of fin mesenchyme demonstrates that zebrafish trunk neural crest does not generate ectomesenchyme. *Development* 2013;140:2923-32.
- McCloy RA, Rogers S, Caldon CE, Lorca T, Castro A, Burgess A. Partial inhibition of Cdk1 in G 2 phase overrides the SAC and decouples mitotic events. *Cell Cycle* 2014;13:1400-12.
- Chatani M, Takano Y, Kudo A. Osteoclasts in bone modeling, as revealed by in vivo imaging, are essential for organogenesis in fish. *Dev Biol* 2011;360:96-109.
- Parichy DM, Ransom DG, Paw B, Zon LI, Johnson SL. An orthologue of the kit-related gene fms is required for development of neural crest-derived xanthophores and a subpopulation of adult melanocytes in the zebrafish, *Danio rerio*. *Development* 2000;127:3031-44.
- Gavaia PJ, Simes DC, Ortiz-Delgado JB, Viegas CS, Pinto JP, Kelsh RN, et al. Osteocalcin and matrix Gla protein in zebrafish (*Danio rerio*) and Senegal sole (*Solea senegalensis*): comparative gene and protein expression during larval development through adulthood. *Gene Expr Patterns* 2006;6:637-52.
- Hammond CL, Schulte-Merker S. Two populations of endochondral osteoblasts with differential sensitivity to Hedgehog signalling. *Development* 2009;136:3991-4000.
- Phan QT, Tan WH, Liu R, Sundaram S, Buettner A, Kneitz S, et al. Cxcl9l and Cxcr3.2 regulate recruitment of osteoclast progenitors to bone matrix in a medaka osteoporosis model. *Proc Natl Acad Sci USA* 2020;117:19276-86.
- To TT, Witten PE, Renn J, Bhattacharya D, Huisseune A, Winkler C. Rankl-induced osteoclastogenesis leads to loss of mineralization in a medaka osteoporosis model. *Development* 2012;139:141-50.
- Kague E, Witten PE, Soenens M, Campos CL, Lubiana T, Fisher S, et al. Zebrafish sp7 mutants show tooth cycling independent of attachment, eruption and poor differentiation of teeth. *Dev Biol* 2018;435:176-84.
- Huisseune A, Van der heyden C, Sire JY. Early development of the zebrafish (*Danio rerio*) pharyngeal dentition (Teleostei, Cyprinidae). *Anat Embryol (Berl)* 1998;198:289-305.

Received for publication: 14 December 2021. Accepted for publication: 8 March 2022.

This work is licensed under a Creative Commons Attribution-NonCommercial 4.0 International License (CC BY-NC 4.0).

©Copyright: the Author(s), 2022

Licensee PAGEPress, Italy

*European Journal of Histochemistry* 2022; 66:3369

doi:10.4081/ejh.2022.3369